Molecular Cell, Volume *79*

Supplemental Information

Homogeneous Oligomers of Pro-apoptotic BAX Reveal Structural Determinants of Mitochondrial Membrane Permeabilization

Zachary J. Hauseman, Edward P. Harvey, Catherine E. Newman, Thomas E. Wales, Joel C. Bucci, Julian Mintseris, Devin K. Schweppe, Liron David, Lixin Fan, Daniel T. Cohen, Henry D. Herce, Rida Mourtada, Yael Ben-Nun, Noah B. Bloch, Scott B. Hansen, Hao Wu, Steven P. Gygi, John R. Engen, and Loren D. Walensky

A

Detergent	Molecular Weight (g/mol)	Critical Micelle Concentration (mM)
n-Dodecylphosphocholine (Fos-12)	351.5	1.5
n-Decyl-β-D-maltoside (DM)	482.6	1.8
n-Dodecyl-β-D-maltoside (DDM)	510.6	0.17
n,n-dimethyl-n-dodecylamine-n-oxide (LDAO)	229.4	1
3-((3-cholamidopropyl) dimethyl ammonio)-1-propanesulfonate (CHAPS)	614.9	8

B

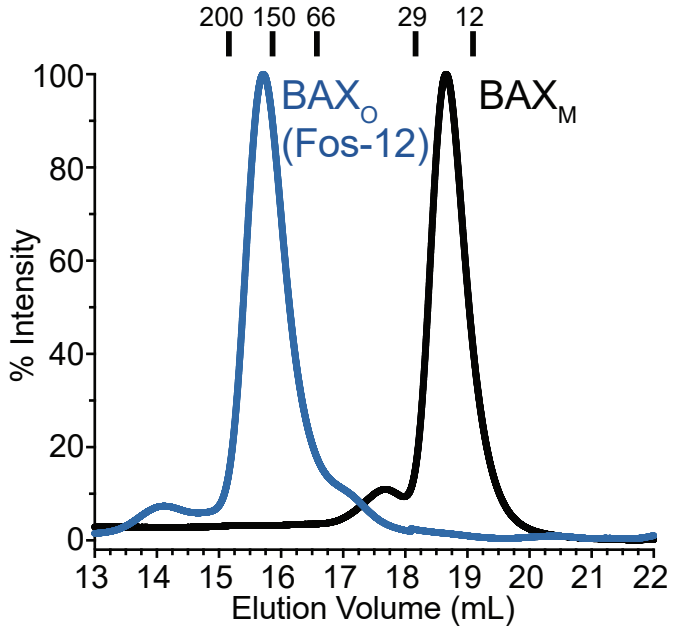

C

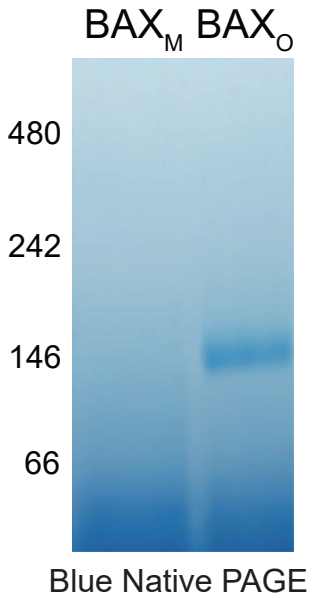

D

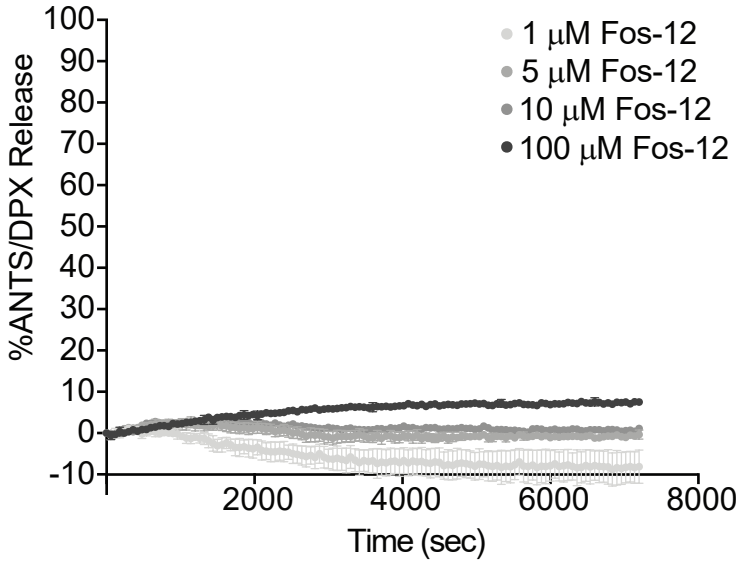

Figure S1

Figure S1, Related to Figure 1. Production of BAX_O at submicellar concentrations of Fos-12 and stability of the generated species in the absence of detergent.

(A) Characteristics of detergents screened for induction of BAX oligomerization.

(B) SEC analysis of BAX_M and BAX_O generated by treatment of BAX_M with submicellar concentration of Fos-12 (1 mM).

(C) Blue native PAGE analysis of BAX_M and Fos-12 induced BAX_O isolated in the absence of detergent, demonstrating the stability of the oligomeric band migrating at ~146 kDa.

(D) Treatment of liposomes with the indicated doses of Fos-12. Error bars are mean ± SEM for liposomal release experiments performed in technical triplicate, with data representative of two independent experiments.

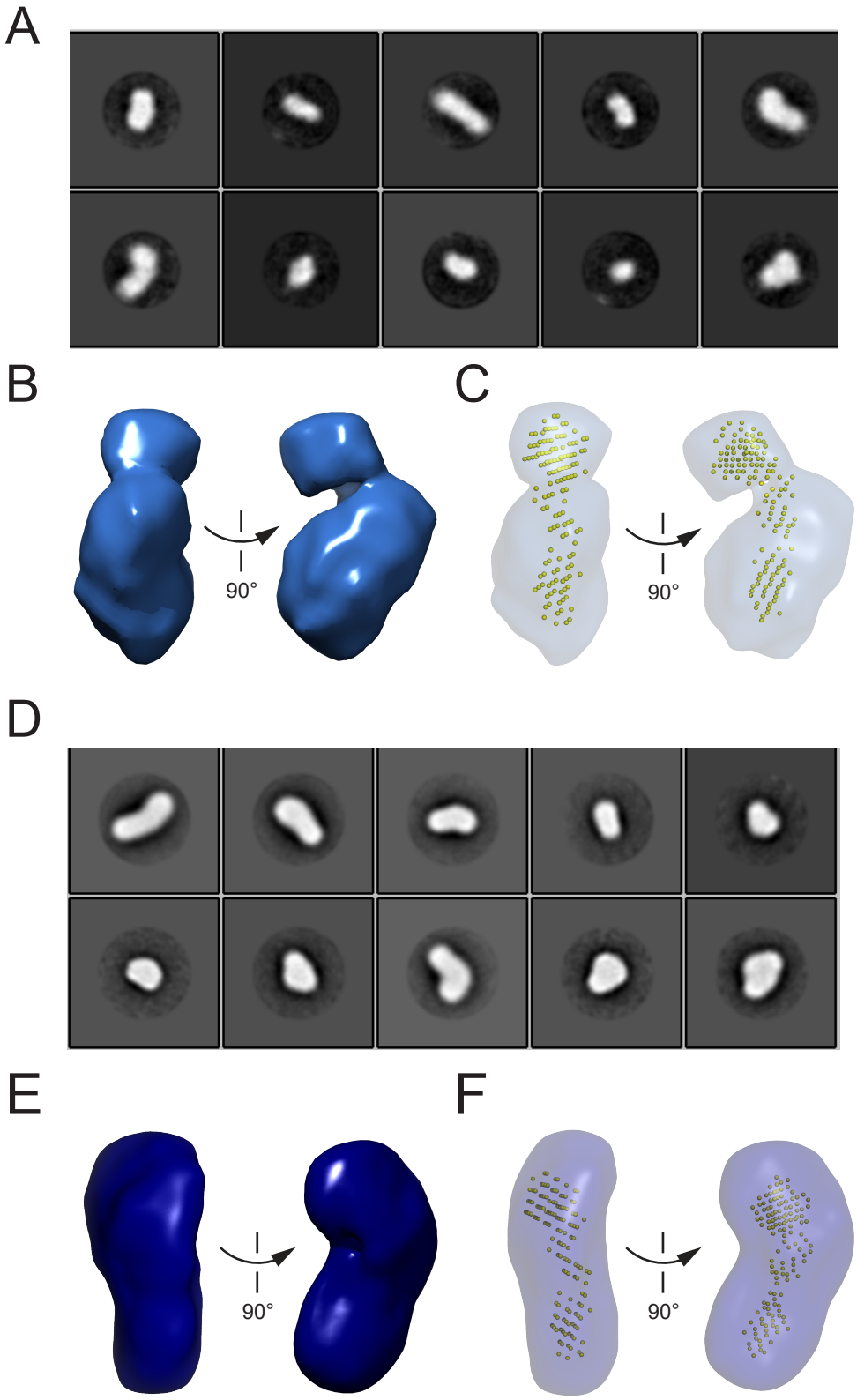

Figure S2

Figure S2, Related to Figure 1. Negative stain EM reveals the curvilinear structure of BAX_O.

(A-C) Two-dimensional classification of negative stain EM of Fos-12-induced BAX_O (A) and the derived three-dimensional reconstruction (B) match the curvilinear envelope derived from SAXS analysis (C).

(D-F) Two-dimensional classification (D) and three-dimensional reconstruction of BAX_O (E) generated by an alternative method, namely BIM $SAHB_{A2}$-triggered BAX_M in the presence of liposomes followed by BAX_O extraction, likewise yielded a curvilinear macromolecular structure, mirroring the size and shape of the species observed by SAXS (F) and EM analyses of Fos-12-induced BAX_O (A-C).

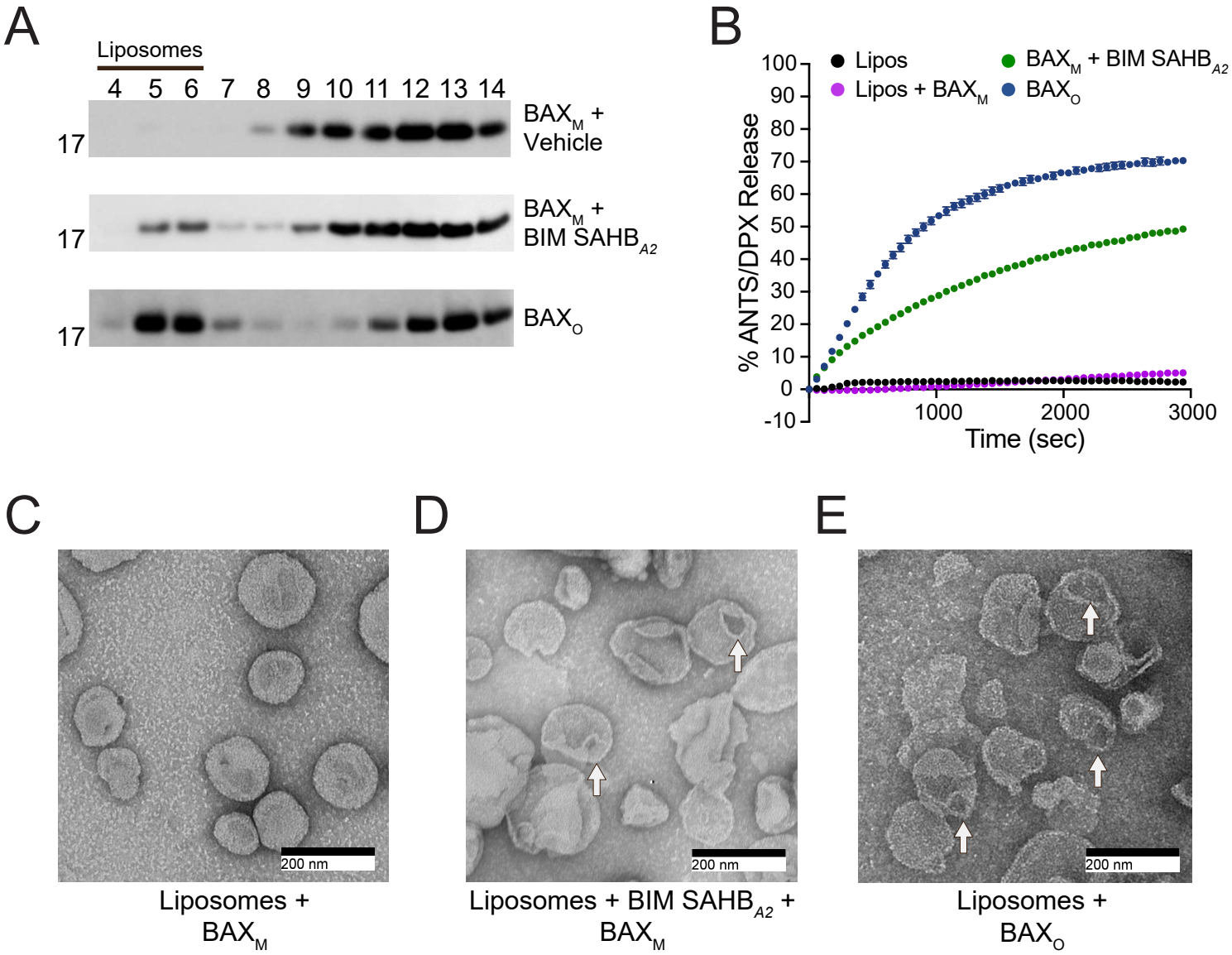
A
Liposomes
4 5 6 7 8 9 10 11 12 13 14
17
BAX$_M$ + Vehicle
17
BAX$_M$ + BIM SAHB$_{A2}$
17
BAX$_O$
B
Lipos
Lipos + BAX$_M$
BAX$_M$ + BIM SAHB$_{A2}$
BAX$_O$
% ANTS/DPX Release
100
90
80
70
60
50
40
30
20
10
0
-10
1000
2000
3000
Time (sec)
C
200 nm
Liposomes + BAX$_M$
D
200 nm
Liposomes + BIM SAHB$_{A2}$ + BAX$_M$
E
200 nm
Liposomes + BAX$_O$

Figure S3

Figure S3, Related to Figure 2. Comparative membrane translocation, liposomal release, and morphology of BAX_M, BIM $SAHB_{A2}$-triggered BAX_M, and BAX_O treated liposomes.

(A) Both BAX_O and BIM $SAHB_{A2}$-triggered BAX_M translocate to liposomes, whereas the totality of vehicle-treated BAX_M remains in the soluble fraction, as monitored by liposomal translocation assay and BAX western analysis. Liposomal fractions (4-6) are marked with an overlying black bar, with supernatant fractions to the right (7-14). The data shown are representative of two independent biological replicates. BAX_M, 500 nM; BAX_O, 500 nM; BIM $SAHB_{A2}$, 500 nM.

(B) BAX_O and BIM $SAHB_{A2}$-triggered BAX_M induce liposomal poration, as assessed by liposomal release assay. Error bars are mean ± SEM for liposomal release experiments performed in technical triplicate, with data representative of two independent experiments. BAX_M, 500 nM; BAX_O, 500 nM; BIM $SAHB_{A2}$, 500 nM.

(C-E) Negative stain electron micrographs of liposomes incubated with BAX_M (C), BIM $SAHB_{A2}$-triggered BAX_M (D), or BAX_O (E), highlighting the similar morphology of membrane disruption induced by BH3-triggered BAX_M and BAX_O in the liposomal membranes.

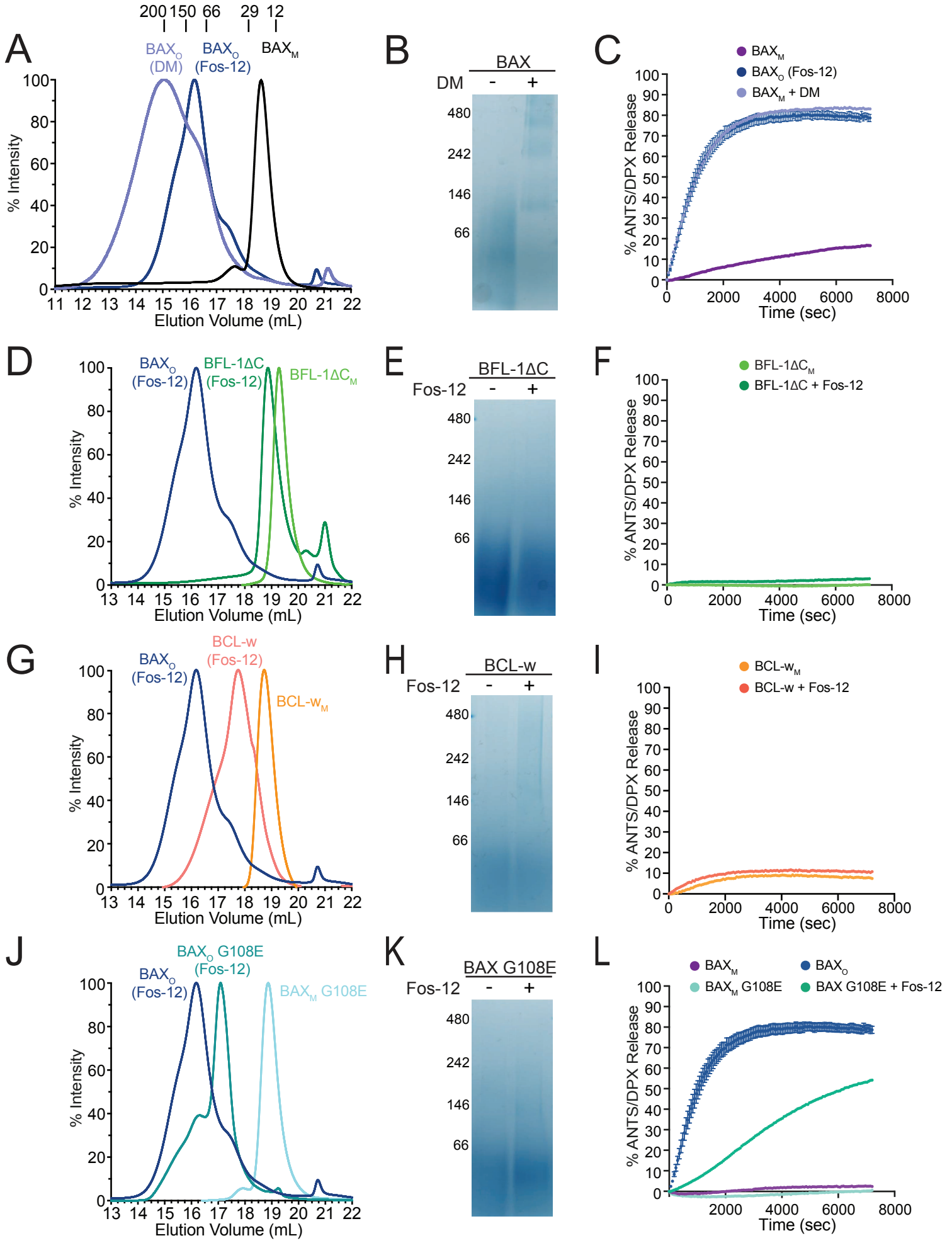
A
200 150 66 29 12
BAXO (DM)
BAXO (Fos-12)
BAXM
% Intensity
Elution Volume (mL)
B
BAX
DM - +
480
242
146
66
C
BAXM
BAXO (Fos-12)
BAXM + DM
% ANTS/DPX Release
Time (sec)
D
BAXO (Fos-12)
BFL-1ΔC (Fos-12)
BFL-1ΔCM
% Intensity
Elution Volume (mL)
E
BFL-1ΔC
Fos-12 - +
480
242
146
66
F
BFL-1ΔCM
BFL-1ΔC + Fos-12
% ANTS/DPX Release
Time (sec)
G
BAXO (Fos-12)
BCL-w (Fos-12)
BCL-wM
% Intensity
Elution Volume (mL)
H
BCL-w
Fos-12 - +
480
242
146
66
I
BCL-wM
BCL-w + Fos-12
% ANTS/DPX Release
Time (sec)
J
BAXO (Fos-12)
BAXO G108E (Fos-12)
BAXM G108E
% Intensity
Elution Volume (mL)
K
BAX G108E
Fos-12 - +
480
242
146
66
L
BAXM
BAXO
BAXM G108E
BAX G108E + Fos-12
% ANTS/DPX Release
Time (sec)

Figure S4

Figure S4, Related to Figure 2. A series of control experiments further validate the fidelity of Fos-12-induced BAX_O.

(A) Comparative SEC analysis of BAX species generated upon treatment of full-length BAX monomer (BAX_M) with DM or Fos-12. The data shown are representative of two independent biological replicates.

(B) Blue native PAGE of BAX_M and DM-induced BAX oligomers, demonstrating the heterogeneity of the resultant species. The data shown are representative of two independent biological replicates.

(C) Fos-12-induced BAX_O and DM-induced BAX oligomers demonstrate comparable membrane poration activity, as assessed by liposomal release assay. Error bars are mean ± SEM for liposomal release experiments performed in technical triplicate, with data representative of two independent experiments. BAX oligomeric protein, 500 nM.

(D) Comparative SEC analysis of BFL-1ΔC, Fos-12-treated BFL-1ΔC, and Fos-12-induced BAX_O.

(E) Blue native PAGE of BFL-1ΔC and Fos-12-treated BFL-1ΔC. The data shown are representative of two independent biological replicates.

(F) Fos-12-treated BFL-1ΔC showed no membrane poration activity, as assessed by liposomal release assay. Error bars are mean ± SEM for liposomal release experiments performed in technical triplicate, with data representative of two independent experiments. BFL-1ΔC protein, 500 nM.

(G) Comparative SEC analysis of full-length BCL-w, Fos-12-treated BCL-w, and Fos-12-induced BAX_O. The data shown are representative of two independent biological replicates.

(H) Blue native PAGE of BCL-w and Fos-12-treated BCL-w. The data shown are representative of two independent biological replicates.

(I) Fos-12-treated BCL-w showed no membrane poration activity, as assessed by liposomal release assay. Error bars are mean ± SEM for liposomal release experiments performed in technical triplicate, with data representative of two independent experiments. BCL-w protein, 500 nM.

(J) Comparative SEC analysis of BAX_M G108E, Fos-12-treated BAX G108E, and Fos-12-induced BAX_O. The data shown are representative of two independent biological replicates.

(K) Blue native PAGE of BAX_M G108E and Fos-12-treated BAX G108E. The data shown are representative of two independent biological replicates.

(L) Fos-12-treated BAX G108E demonstrated impaired membrane poration activity as compared to Fos-12-induced BAX_O in liposomal release assays. Error bars are mean ± SEM for liposomal release experiments performed in technical triplicate, with data representative of two independent experiments. BAX proteins, 500 nM.

A

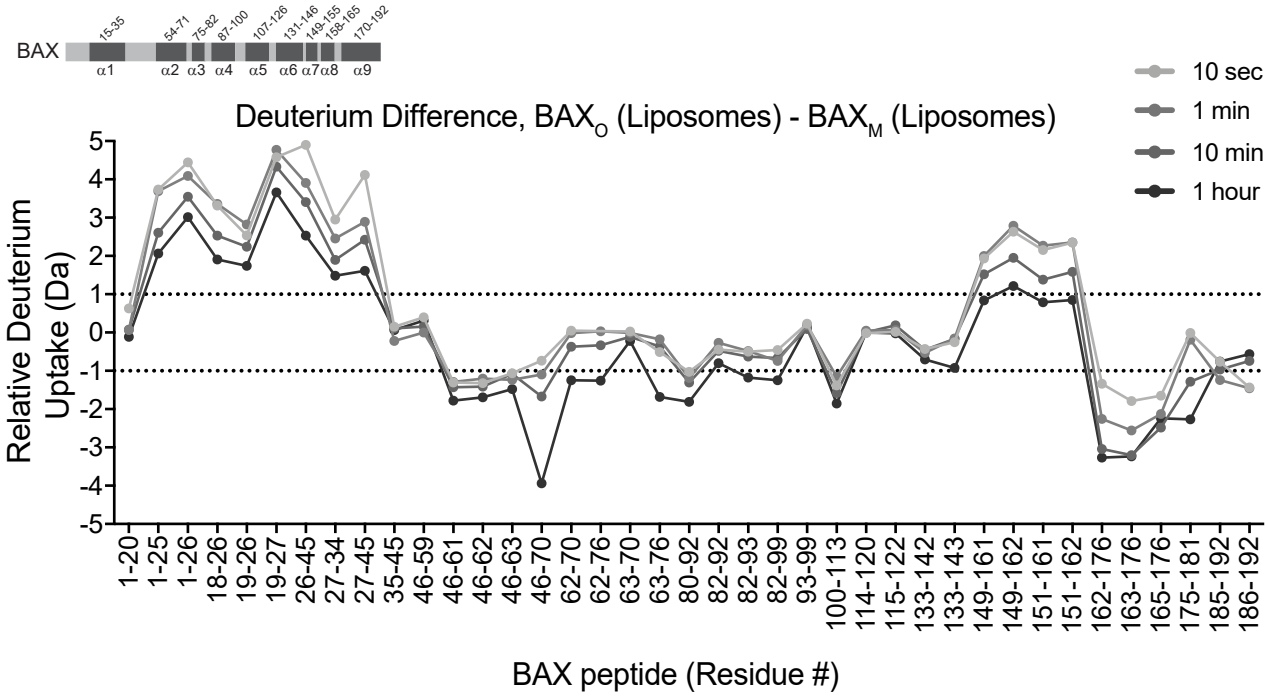

B

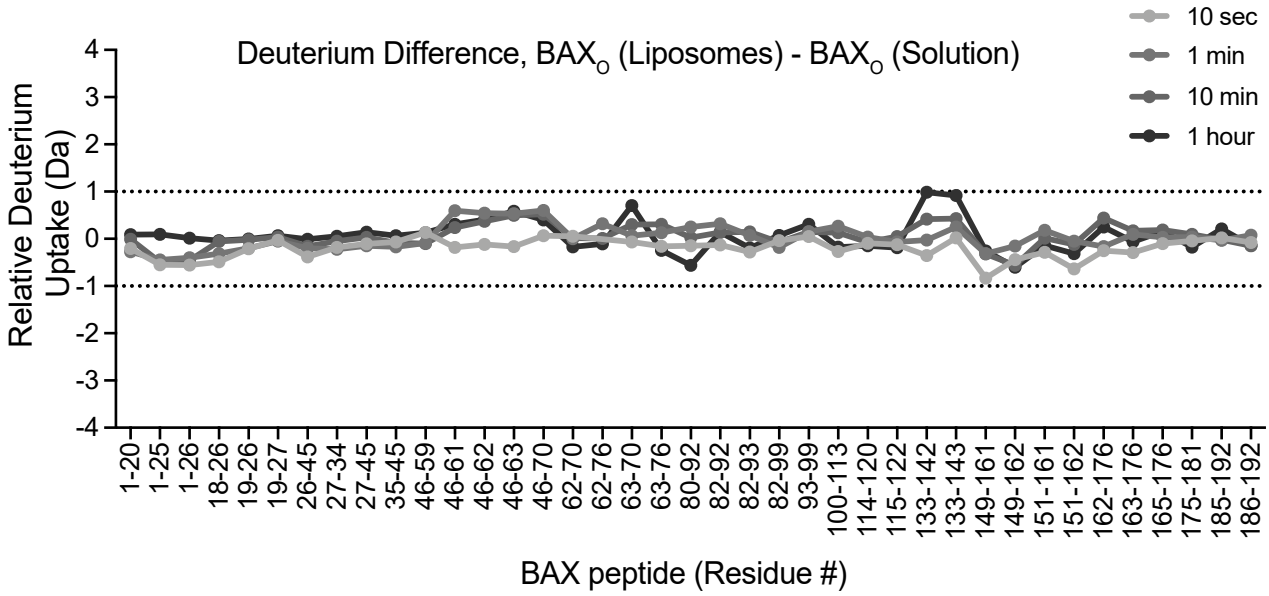

C

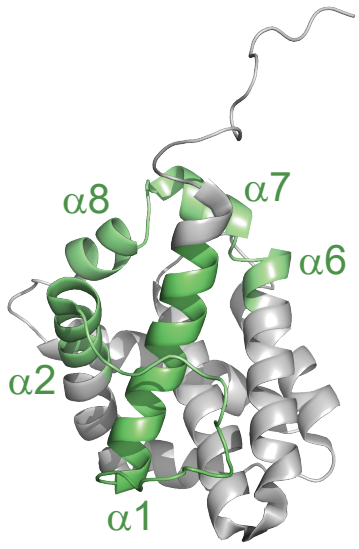

BCL-2 BH4/BAX$_M$ - BAX$_M$

D

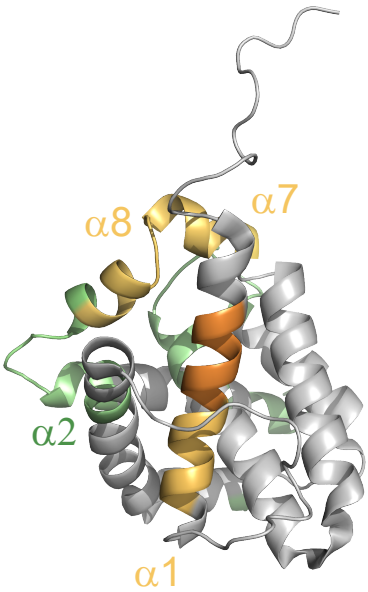

BAX$_O$ - BAX$_M$

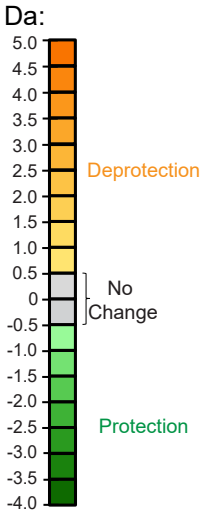

Figure S5

Figure S5, Related to Figure 3. Comparative HXMS analyses of BAX_M vs. BAX_O in the membrane environment, BAX_O in solution vs. the membrane environment, and the inverse HXMS profiles of BAX_O and BCL-2 BH4-inhibited BAX_M.

(A) The difference in deuterium uptake plot demonstrates the relative deuterium incorporation of BAX_O (Figure 3B) minus the relative deuterium incorporation of BAX_M (Figure 3A), as measured at the indicated time points in the presence of liposomes. The regions of conformational deprotection upon formation of BAX_O include the N-terminus, α1, and the α7-α8 junction, whereas regions of protection are α2, α4-α5 loop, proximal α5, distal α8, and α9. Dotted lines indicate the boundaries of significant differences in deuteration (± 1.0 Da). Data are representative of two independent experiments.

(B) The deuterium difference plot demonstrates the relative deuterium incorporation of BAX_O in the presence of liposomes minus the relative deuterium incorporation of BAX_O in aqueous solution. The dotted lines indicate the boundaries for significant differences in deuteration (± 1.0 Da), and thus highlight the absence of meaningful, detectable changes in deuterium uptake for BAX_O between the membrane and aqueous conditions. Data are representative of two independent experiments.

(C-D) Comparison of the HXMS profiles of BCL-2 BH4-bound BAX_M (C) and Fos-12 induced BAX_O (D) demonstrate that the conformational deprotection observed upon BAX oligomerization, such as in α1, α7 and α8, are precisely those regions that are restrained upon treatment of BAX_M with a stapled BCL-2 BH4 helix.

See also Table S1.

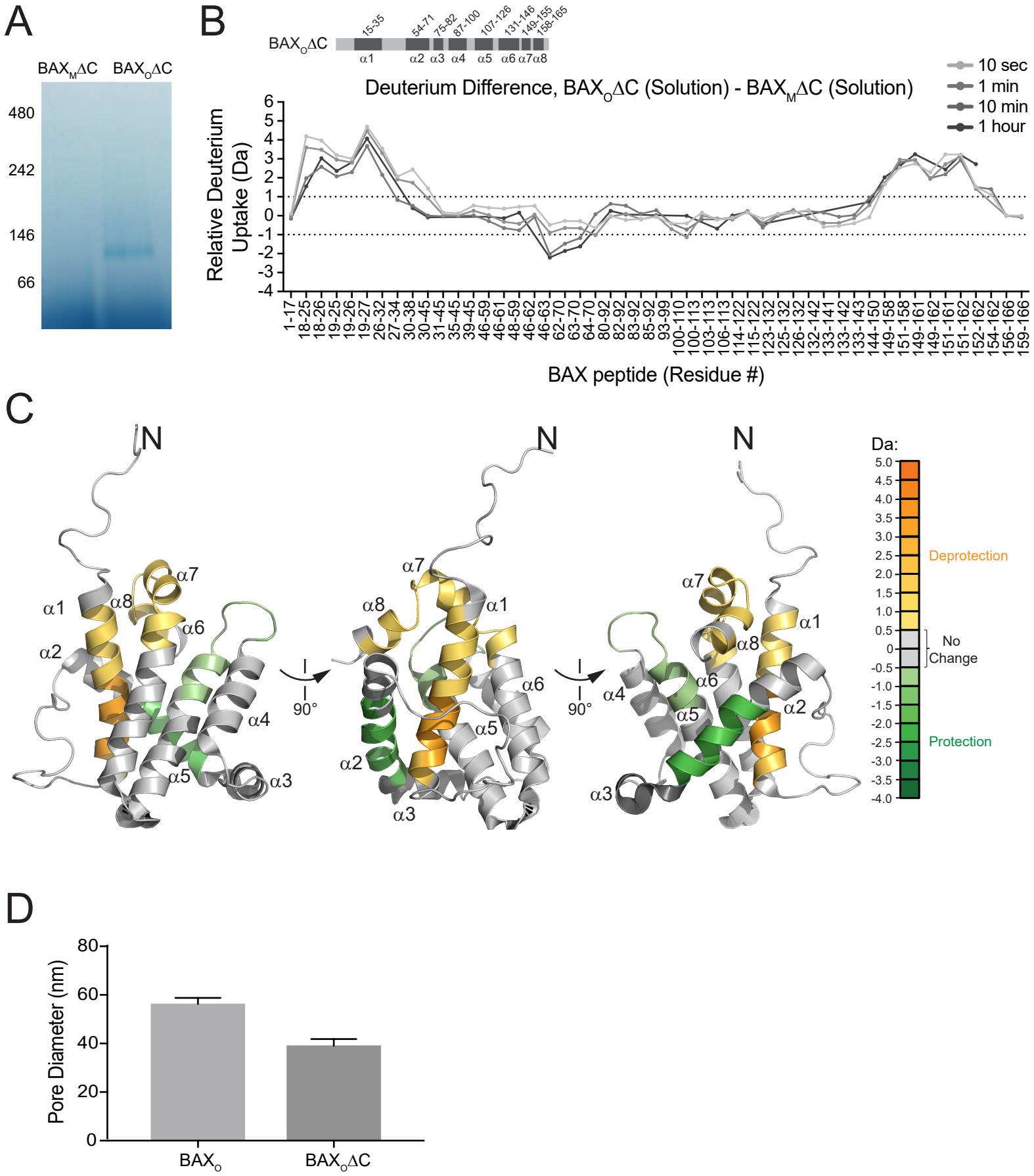
A
BAXMΔC
BAXOΔC
480
242
146
66
B
BAXOΔC
15-35
54-71
75-82
87-100
107-126
131-146
149-155
158-165
α1
α2
α3
α4
α5
α6
α7
α8
Deuterium Difference, BAXOΔC (Solution) - BAXMΔC (Solution)
10 sec
1 min
10 min
1 hour
Relative Deuterium Uptake (Da)
BAX peptide (Residue #)
C
N
90°
Da:
Deprotection
No Change
Protection
D
Pore Diameter (nm)
BAXO
BAXOΔC

Figure S6

Supplementary Figure S6, Related to Figure 6. Comparative HXMS analysis of $BAX_M\Delta C$ and $BAX_O\Delta C$, and quantitation of liposomal poration by BAX_O vs. $BAX_O\Delta C$.

(A) Blue native PAGE of $BAX_M\Delta C$ and Fos-12-induced $BAX_O\Delta C$, showing the conversion of monomeric BAXΔC into a single oligomeric band migrating at ~120 kDa. The data shown are representative of two independent biological replicates.

(B) The deuterium difference plot demonstrates the relative deuterium incorporation of $BAX_O\Delta C$ minus the relative deuterium incorporation of $BAX_M\Delta C$ in aqueous solution. The dotted lines indicate the boundaries for significant differences in deuteration (± 1.0 Da). Data are representative of two independent biological replicates.

(C) The prominent regions of conformational deprotection and protection upon conversion of $BAX_M\Delta C$ to $BAX_O\Delta C$ are mapped onto the monomeric structure of BAX (PDB: 1F16) according to the orange and green color scale, and reflect a similar HXMS profile to that observed for the conversion of BAX_M to BAX_O (Figures 3, S5A).

(D) Mean pore size observed in LUVs treated with BAX_O or $BAX_O\Delta C$ for 15 min. Error bars are mean ± SEM for BAX_O (n=81) and $BAX_O\Delta C$ (n=53) pores counted. At 15 min, 84% and 30% of the liposomes were porated/disrupted upon treatment with BAX_O or $BAX_O\Delta C$, respectively.

See also Table S2.

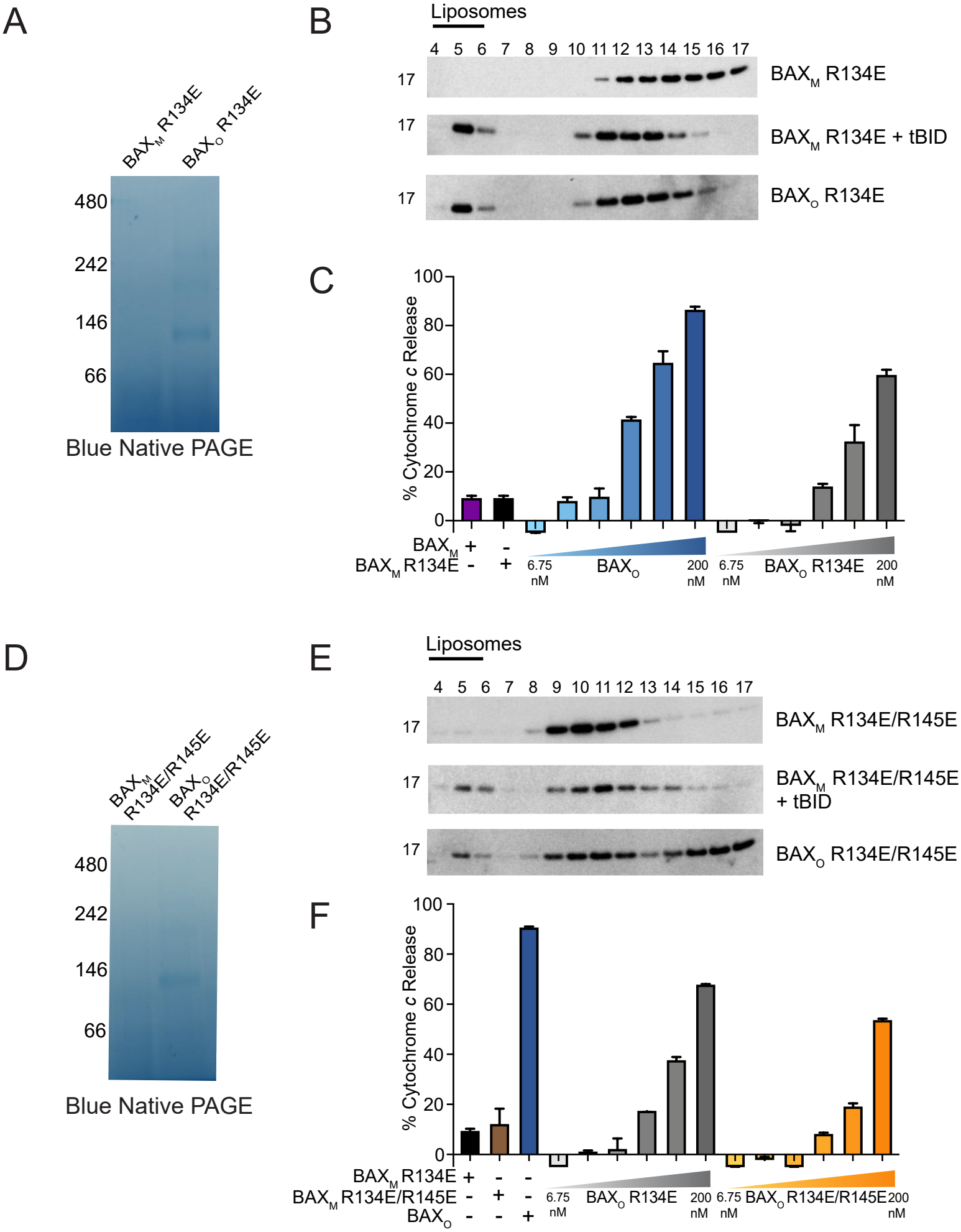
A
BAXM R134E
BAXO R134E
480
242
146
66
Blue Native PAGE
B
Liposomes
4 5 6 7 8 9 10 11 12 13 14 15 16 17
17
BAXM R134E
BAXM R134E + tBID
BAXO R134E
C
% Cytochrome c Release
100
80
60
40
20
0
BAXM +
BAXM R134E -
6.75 nM
BAXO
200 nM
BAXO R134E
D
BAXM R134E/R145E
BAXO R134E/R145E
Blue Native PAGE
E
BAXM R134E/R145E
BAXM R134E/R145E + tBID
BAXO R134E/R145E
F
BAXM R134E +
BAXM R134E/R145E -
BAXO -
BAXO R134E
BAXO R134E/R145E

Figure S7

Supplementary Figure S7, Related to Figure 7. Mutagenesis of conserved arginines in the amphipathic BAX α6 helix impairs mitochondrial membrane permeabilization by BAX_O.

(A) Blue native PAGE of BAX_M R134E and Fos-12-induced BAX_O R134E, demonstrating the conversion of monomeric BAX R134E into a single oligomeric band migrating at ~146 kDa.

(B) Comparative membrane translocation of tBID-triggered BAX R134E and BAX_O R134E, as monitored by liposomal translocation assay and BAX western analysis. Liposomal fractions are marked with an overlying black bar (4-6), with supernatant fractions (7-17) to the right. The data shown are representative of two independent biological replicates.

(C) Comparative dose-responsive cytochrome *c* release upon treatment of BAX/BAK-deficient mouse liver mitochondria with BAX_O or BAX_O R134E. Error bars are mean ± SEM for cytochrome *c* release experiments performed in technical triplicate, with data representative of two independent experiments. BAX_M and BAX_M R134E, 200 nM; BAX_O and BAX_O R134E, 6.25-200 nM.

(D) Blue native PAGE analysis of BAX_M R134E/R145E and Fos-12-induced BAX_O R134E/R145E, demonstrating the conversion of monomeric BAX R134E/R145E into a single oligomeric band migrating at ~146 kDa.

(E) Comparative membrane translocation of tBID-triggered BAX_M R134E/R145E and BAX_O R134E/R145E, as monitored by liposomal translocation assay and BAX western analysis. Liposomal fractions are marked with an overlying black bar (4-6), with

supernatant fractions (7-17) to the right. The data shown are representative of two independent biological replicates.

(F) Comparative dose-responsive cytochrome *c* release upon treatment of BAX/BAK-deficient mouse liver mitochondria with BAX_O R134E or BAX_O R134E/R145E. Error bars are mean ± SEM for cytochrome *c* release experiments performed in technical triplicate, with data representative of two independent experiments. BAX_M R134E and BAX_M R134E/R145E, 200 nM; BAX_O R134E and BAX_O R134E/R145E, 6.25-200 nM.

Data Set	BAX_M	BAX_M + liposomes	BAX_O	BAX_O + liposomes
HDX reaction details [a]	Final D_2O concentration = 92.3%, pH_{read} = 6.60, 21 °C			
HDX time course	0.167, 1, 10, and 60 minutes			
HDX controls	6 undeuterated controls, at least one for each state			
Back-exchange	30-35%			
Number of peptides [b]	80 identified, 39 followed coincident in all 4 states			
Sequence coverage[c]	89.1%			
Average peptide length[c] **Redundancy**[c]	Average length: 13.21 Redundancy: 3.01			
Replicates	2 biological replicates, 2 technical replicates of each biological			
Repeatability	+/- 0.25 relative Da			
Meaningful differences	$\geq$ 1.0 Da			

[a] 12-fold dilution with labeling buffer [10 mM HEPES, 200 mM KCl, 1 mM $MgCl_2$, pD 7.0]. 1-fold dilution with quench buffer [0.8 M GdmCl, 0.8% FA pH 2.5].

[b] Parameters to filter peptides for identification from the 6 undeuterated controls were: 4 consecutive products, 0.4 fragmentation products per amino acid, 10 ppm error.

[c] Calculated for those peptides that were coincident in all 4 states for comparative analyses.

Table S1

Table S1, Related to Figure 3. Data summary and list of experimental parameters for HXMS analyses of BAX_M and BAX_O.

Data Set	$BAX_M\Delta C$	$BAX_O\Delta C$
HDX reaction details [a]	Final D_2O concentration = 94.7%, pH_{read} = 6.60, 21 °C	
HDX time course	0.167, 1, 10, and 60 minutes	
HDX controls	4 undeuterated controls, 2 for each state	
Back-exchange	30-35%	
Number of peptides [b]	85 identified, 50 followed coincident in both states	
Sequence coverage[c]	94.6%	
Average peptide length[c] **Redundancy**[c]	Average length: 10.44 Redundancy: 3.32	
Replicates	2 biological replicates, 1 technical replicate of each biological	
Repeatability	+/- 0.25 relative Da	
Meaningful differences	$\geq$ 1.0 Da	

[a] 18-fold dilution with labeling buffer [10 mM HEPES, 200 mM KCl, 1 mM $MgCl_2$, pD 7.0]. 1-fold dilution with quench buffer [0.8 M GdmCl, 0.8% FA pH 2.5].

[b] Parameters to filter peptides for identification from the 4 undeuterated controls were: 1 consecutive products, 0.25 fragmentation products per amino acid, 10 ppm error.

[c] Calculated for those peptides that were coincident in both states for comparative analyses.

Table S2

Table S2, Related to Figures 6 and S6. Data summary and list of experimental parameters for HXMS analyses of $BAX_M\Delta C$ and $BAX_O\Delta C$.